Using blister test to predict the failure pressure in bonded composite repaired pipes

Silvio DE BARROS, B.M. Fadhil, Fahmi Alila, J. Diop, J.M.L. Reis, Pascal Casari, Frédéric Jacquemin

aUsing blister test to predict the failure pressure in bonded composite repaired pipes

S. de Barros[1,3], B.M. Fadhil[2,3], F. Alila[3], J. Diop[3], J.M.L. Reis[4], P. Casari[3], F. Jacquemin[3].

[1]Federal Center of Technological Education in Rio de Janeiro, Brazil.

[2]Koya University, Erbil, Iraq.

[3]Université de Nantes, Institut de Recherche en Génie Civil et Mécanique, Saint-Nazaire, France

[4] Universidade Federal Fluminense, Mechanical Engineering Department, Rio de Janeiro, Brazil

Abstract

The design and qualification of composite repairs for pipelines usually requires hydrostatic tests for the determination of the failure pressure. In this work, the use of a shaft blister test to assess the failure pressure of composite repairs is proposed. Blister tests were conducted to investigate the interfacial debonding of a composite plate bonded to steel substrate. The blister test specimen represents a composite repair applied to a pipeline with a defect. The onset debonding load is used to predict the failure pressure. A 3D digital image correlation (DIC) has been used to follow up the debonding propagation and evaluate the blister shape. 3D finite element model with a cohesive zone model has been used to simulate loaded shaft blister test. A good correlation between blister tests results and finite element simulation results was obtained. The validated finite element model was used to predict failure pressure in bonded composite repaired pipes with different values of defect diameter and repair thickness. The results show that the blister test could replace hydrostatic tests for the analysis of the composite repairs performance.

Keywords: composite repair, blister test, failure pressure

1. Introduction

The composite material has entered the industry of the widest doors in all fields. Currently, it has become a strong alternative to repair systems for several reasons, such us: its resistance to corrosion, rapid repair, safety as well as its distinctive economic cost [1]. These repair systems have begun to be rapidly developed, especially in the oil industry, including the repair of pipes. As a result of the extension of the oil pipelines to hundreds of kilometers in different environments and sever conditions such as high temperature and presence of sand in Arabic deserts and to very low temperature like in Siberia, this which could the external conditions. Since these pipelines are made of steel, it will suffer from corrosion and erosion due to the physical properties of the oil. As time passes, harsh deterioration of pipelines might be encountered. Holes and pits are common defects as a result of material's wear; such defects may cause leakage in the pipelines. These defects must be repaired to protect the proper functioning of plants [2]. Many researchers have carried out studies on repairing metal pipes with composite materials from [3].

Repairing with composites patch and wrapped composite are used extensively for its excellent performance against the stresses generated within the pipes as well as restoring the bending and tensile stiffness of the pipelines as a result of high internal pressure [4,5]. Composite repairs might be outstanding over other materials repairs for their good fatigue performance, stiffness, corrosion resistance, weight reduction and thermal insulation [6]. Wrapped composite repairs made of carbon or glass fiber reinforcements with epoxy matrix resins are used as well as pre-cured composite like hard-shells [7] and stand-off clamps [8]. Interfacial characterization has an important role in composite repairs performance and behavior. Delamination is the most important failure mode between layers in the repair/metal substrate interface after the transferred fluid has infringed through the pipeline wall forming a blister [9]. The delamination in the blister test is reached by low strain, so the results of the test are more important to the adhesion of the composite repair [10]. Dannenberg [11] was the first to suggest the blister test. Many tests have been developed to find the adhesion toughness of a thin film to, for example, peeling tests [12], scratching tests [13] and indentation tests [14]. Blister tests are widely used in different fields and further developed by Jensen [15,16]. In addition, several mathematical models have been developed to match the adhesion stiffness of films with the blister which is produced by either a point load or pressure load [17–19]. Blister test has been used to evaluate the mechanical resistance of brazing joints between ceramic and metal, [20]. The effect of the shaft head on the energy release rate has been investigated. The results have been compared with blister test by using fluid pressure, mathematical solution was presented as well [21]. A theoretical investigation of the elastic strain energy presented by determining the film/substrate interface [22]. Shaft loaded blister tests were conducted to determine the interfacial failure of composite coating material adhesively bonded to a metal substrate. The environmental control was performed to investigate its impact on the total energy release rate [23]. The total energy release rate G_T can be obtained from the failure load F.

$$G_T = \frac{F^2}{32\pi^2 D} \quad (1)$$

Where D is the bending stiffness calculated according to the equivalent properties of the laminate, Young's modulus E and Poison's ratio ν, and plate thickness t.

$$D = \frac{Et^3}{12(1-\nu^2)} \quad (2)$$

The standards ISO/TS 24817 [24] and ASME PCC-2 [25] present the Eq. 3, from which it is possible to assess the failure pressure P in composite repaired pipes:

$$P = \sqrt{\frac{G_T}{\frac{(1-\nu^2)}{Eac}\left(\frac{3}{512t^3}d^4+\frac{1}{\pi}d\right)+\frac{3}{64Gt}d^2}} \quad (3)$$

Where d is the hole diameter and G is the equivalent shear modulus.

Kopple et al. [26] proposed an improved equation to assess the failure pressure but the standard equation is applied here because it uses a combined Young's modulus $E_{ac} = \sqrt{E_{11} \cdot E_{22}}$ to consider a quasi-isotropic material behavior.

Hydrostatic tests, normally used to qualification and design of composite repairs for pipelines, require facilities with special security concerns. Furthermore, these tests use huge specimens prepared with a section cut from the real pipes. In this work, the use of a shaft blister test to assess the failure pressure of composite repairs is investigated. In a similar work, Alnaser and Keller [27] have used Width Tapered Double Cantilevered Beam (WTDCB) tests for obtaining the critical fracture energy value than assess the failure pressure. Blister tests and numerical simulations are used here to show that blister can provide a more accurate assessment of the failure pressure.

2. Materials and methods

2.1. Blister test

The blister test was performed using a universal tensile machine with a capacity of 50KN. The plates were placed horizontally and the painted faces positioned down and fixed on the testing machine using four studs. Two CCD cameras were mounted below the specimen to monitor the strain progressing on the surface. The cross head speed was 2mm/min and the force was applied on the punch (shaft). The blister test configuration is shown in Figure 1. The use of a shaft makes the Blister test far less voluminous than using hydrostatic pressure. There is no need of closed pipe to prevent from pressure leaks. Therefore, it is possible to use smaller composite specimen and smaller substrate. This is the major advantage of blister test.

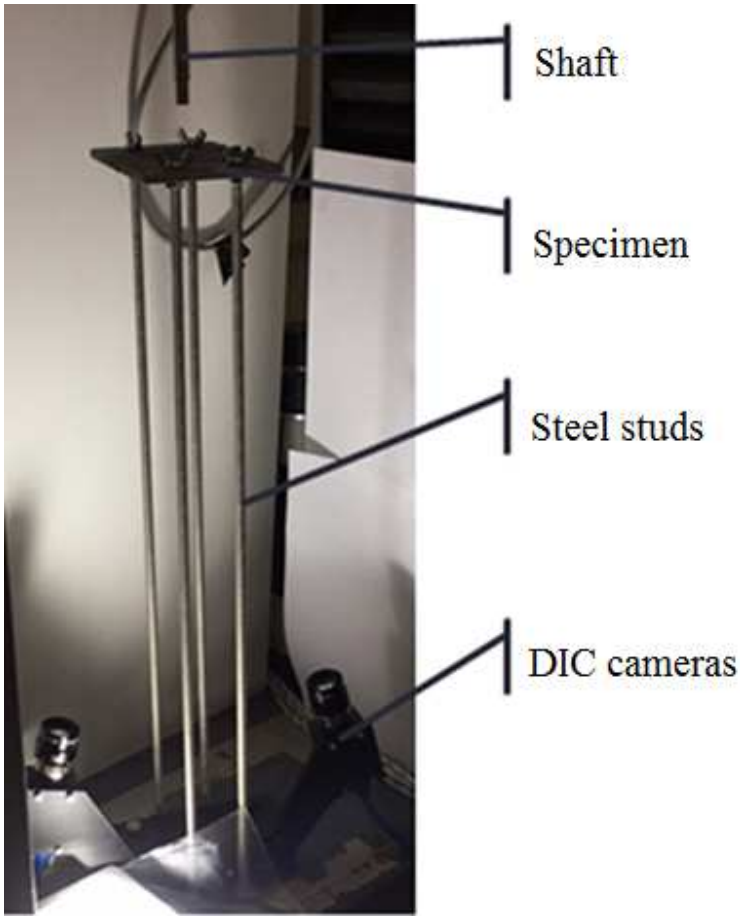

Figure 1. Blister test setup.

2.1.1. Materials

Steel (s355) plates of 6 mm thickness with a chemical composition of 0.23% C, 1.6% Mn, 0.05% Si, 0.05% S, and 0.05% P, an ultimate strength of 470 MPa and yield strength of 355 MPa have been used as substrate.

Composite materials plates with 600x500x1.3 mm dimensions have been manufactured. The plate, consists of 6 woven glass fiber layers [0, 90] and epoxy matrix composed of 70% of resin and 30% of hardener. The mechanical properties are specified in Table 1. The glass fiber layers are stacked on a plastic plate. After laying each layer, the matrix mixing is poured on. With a spatula air bubbles are pushed outside the composite plate. When the composite plate contains no bubble and is transparent and bright, then the layer is well mixed in good proportion with the matrix. If there are still bubbles, they must be taken off. If the plate is not transparent or bright, it means there is not enough matrix mixed with the glass fiber.

Table 1. Equivalent properties of the laminate

Modulus of elasticity E11(GPa)	Modulus of elasticity E22(GPa)	Shear modulus G(GPa)	Poisson's ratio v
20	20	3	0.2

2.1.2. Specimens Preparation

Steel plates with 95 x 140 x 6 mm dimensions were drilled with 4 holes with 9mm diameter to fix the specimen on the testing machine, in the centre of the substrate a 10mm diameter hole is made to permit the shaft to pass through (Figure 2). By using sand blasting technique, the top surface of those plates were prepared to remove any pits or scratches and give a specific roughness. After that, surfaces of the steel plates were cleaned with acetone and piece of cotton cloth in order to completely remove grease or dust. The hole in the center now sealed with molten wax to avoid the glue to penetrate inside. Then the plates were coated with a very thin layer of epoxy adhesive (LOCTITE EA 9483).

Composite material plates with 80 x 80 x 1.3 mm dimension were applied on the steel plates with thin layer of epoxy adhesive and left them at room temperature for 5 days. The final step was to remove the wax form the center hole.

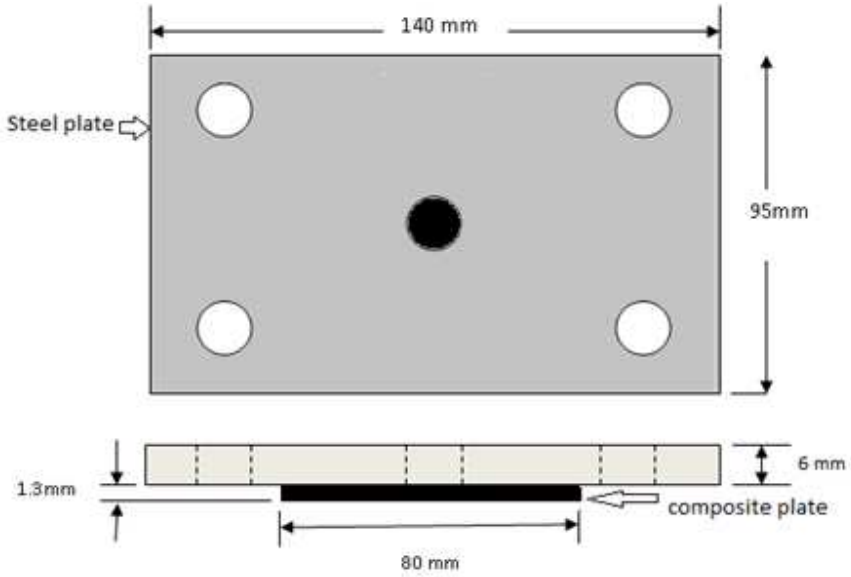

Figure 2. Blister test specimen.

In order to ensure an axisymmetric evolution of the blister during the test, a half ball of steel with 8 mm diameter was glued on the composite material inside the central hole, once the specimens were ready to be tested (Figure 3).

Figure 3. Specimen with the steel half ball placed for the test.

2.1.3. Digital Image Correlation

Optical strain measurements have been widely used to determine the mechanical properties of different materials. These methods are non-contact processes and are particularly suitable for flexible polymeric materials. This provides a physical way to track and locate the movement of multiple facets during the whole strain process. Therefore, every facet can work as a virtual local strain gauge. The quality and accuracy of the measurement are strongly influenced by the visual details of the surface and the contrast. In order to produce fine details and exploitable, usually, a random pattern of paint is applied to the surface of the sample.

A digital image correlation (DIC) technique has been used to follow up the debonding propagation and evaluate the blister shape. By comparing two digital images features of the composite surface before and after deformation, total strain data can be obtained. For this purpose a two-camera system has been used to monitor the strain progressing on the surface. The schematic of DIC technique used for the blister test is shown in Figure 4. With these two cameras, the strain profile of the blister can be captured. The whole surface of the blister can be monitored by the two cameras to evaluate the blister shape.

In order to realize digital image correlation, a speckle has been realized. The chosen speckle was realized with a first layer of white paint a then a second one with a black paint pulverizing random points on the white layer (Figure 5).

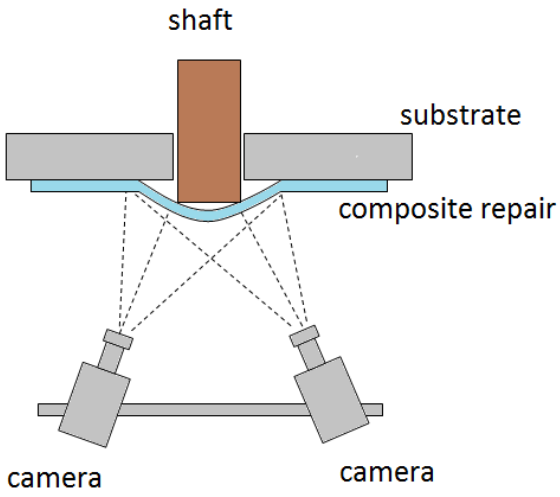

Figure 4. DIC schematic.

Figure 5. Specimen prepared for DIC.

2.1.4. Numerical model

A three-dimensional finite element model was built using ANSYS to simulate the blister test. A Cohesive Zone Model (CZM) was used to represent the interface between the metallic substrate and the composite repair plate. The model implemented in ANSYS is based on a bilinear traction separation law proposed by Alfano and Crisfield [28]. The main parameters of the models are the traction stress (T) and the interfacial displacement δ. SOLID185 element was used for 3D modeling of the solid structures and INTER205 element is an interface element used to simulate the interface between the metal and the composite. Figure 6 shows the finite element model meshing and boundary conditions of the sample. Due to the axisymmetric geometry of the specimen symmetry

boundary conditions were used in order to reduce the run time of the analysis. A fixed displacement was applied on the area of the hole representing the fastening nut and stud. A vertical displacement was applied to the upper keypoint rather than modeling the shaft.

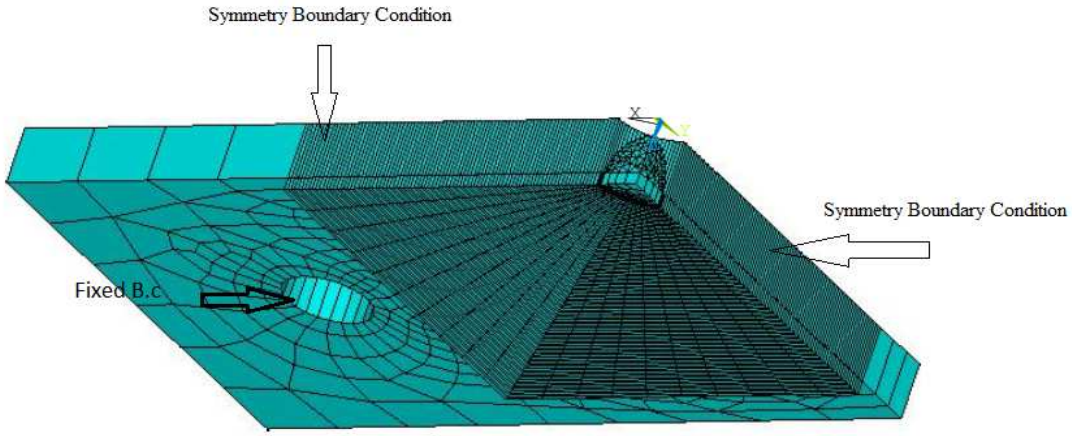

Figure 6. Finite element model.

2.2. Hydrostatic test

Hydrostatic tests with water at room temperature were performed in metallic pipelines with through thickness defects reinforced with composite sleeve repair systems. They are performed to assess information about the effectiveness of a given repair or reinforcement system in a damaged pipeline.

Nine steel pipes with different hole size reinforced with the polyurethane composite repair system was analyzed. The pipe material is an API 5L X65 steel with the following basic properties: Youngs Modulus E_{pipe} = 210 GPa; yield stress σ_y = 450 MPa and ultimate strength σ_u = 627 MPa. The API-5L X65 grade steel is one of the most common pipeline materials in oil industry.

The pipe was prepared for testing by machining different hole sizes, 10 mm, 15 mm and 25 mm, 3 specimens were per each hole size were tested. Before application of the reinforcement, in order to promote a better adhesion between pipe and composite, the pipe surface was prepared using a bristle blaster machine to achieve the roughness level required by the manufacturer (from 25 to 75 μm) and then a primer layer (Subsea® LV) which is a two-part unique blend of liquid epoxy, including Kevlar, polymer and aliphatic polyamine curing agents was used to level the surface and seal the system. The steel pipe was wrapped with concentric layers of a fiberglass tape with water-activated polyurethane resin (Tape Glass®). The fibers are oriented between 0° and 90°. The calculations of Annex D of standard ISO/TS 24817 [24] result in a repair thickness of 0.22″ (5.60 mm – 17 layers with ply thickness of 0.013″) with a 11.81″ (300.0 mm) repair length. Finally, a porous compression film is applied to keep the composite compact during curing time. The porosity in the film is necessary to allow the release of gases during the curing process.

The pipes were closed with a set of welded flanges at both ends, filled with water and then attached to a hydrostatic test machine. The ramp pressure increases approximately 0.1 MPa (1 bar) per second as per defined in ASTM D1599 [29] standard. Pressure increases until a delamination occurs between the composite laminate layers and the substrate. Table 2 presents Tape Glass properties according to the manufacturer.

Table 2 – Tape glass mechanical properties

Modulus of elasticity E11(GPa)	Modulus of elasticity E22(GPa)	Shear modulus G(GPa)	Poisson's ratio v
6,7	6.7	4.54	0.26

3. Results and Discussion

Four specimens were prepared in this work and the load versus vertical displacement of the shaft curves obtained from the blister tests are shown in Figure 7. As it was pointed out by Islam and Tong [23], three regions can be observed. Region 1 is where the critical load of initial debonding of the repair can be observed. Region 2 is where the interfacial debonding propagates and Region 3 is where the final rupture of the repair occurs. The average value of the critical load identified at the end of the Region 1 is used to calculate the total energy release rate (G_T).

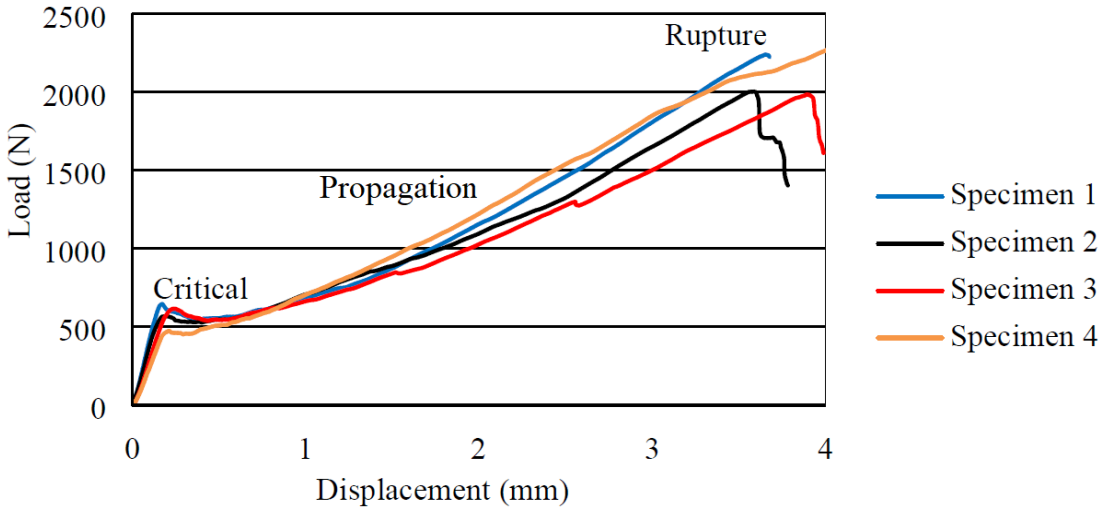

Figure 7. Blister tests - load displacement curves.

Figure 8 shows the 3D profile of the blister obtained by DIC. It can be seen that the blister profile remains quite symmetrical during the debonding propagation until the end of the test.

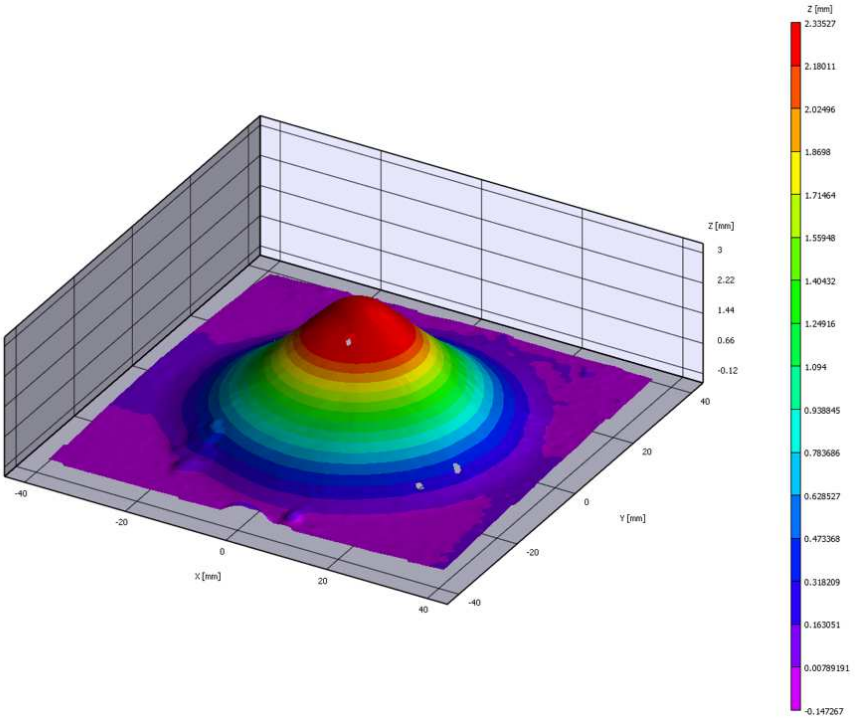

Fig .8. 3D Profile of blister by DIC

Strain on the surface of the sample could be also generated from displacement. Figure 9 shows the strain exy of one specimen at the moment when the displacement is around 1.2 mm and the load level is 790 N. The deformation is quite symmetric regarding the diagonal of the studied surface.

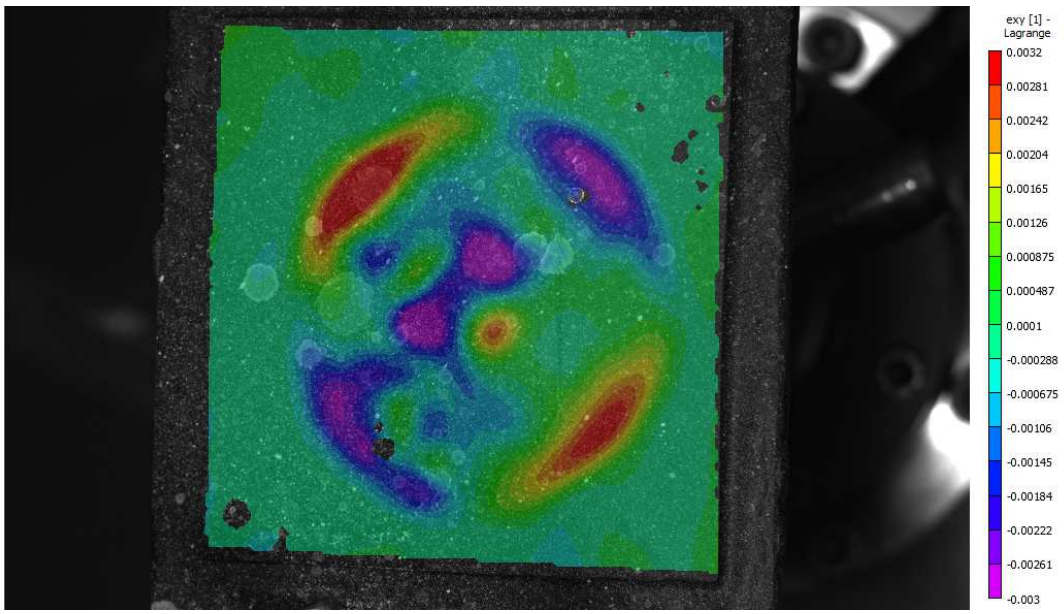

Figure 9. Strain e_{xy} on the surface of the sample.

From the four specimens tested, four values of failure load have been identified, as it can be seen on Table 3. The average critical load is 576 N and it was used to calculate the total energy release rate (G_T). According to eq. 1, the value obtained for G_T was 0.28 N/mm.

Table 3: Measurements of failure load

Specimen	Critical load (N)
1	646
2	567
3	616
4	474
Average	576
Standard deviation	75

This value obtained for G_T was used to assess to corresponding failure pressure according the ISO-Code [24]. Using the diameter of the defect equal to the diameter of the hole in the metallic substrate, it means 10 mm, the Eq. 3 allows to predict a failure pressure of 100 Bar. This value seems to be reliable because it is in a good agreement with hydrostatic test results obtained in a previous experimental work [30]. However, the values cannot be directly compared because the test conditions were different in this previous work. In particular, the temperature during the hydrostatic tests was 80°C while in actual work the test was performed in room temperature. Besides, the repair thicknesses in the previous work were greater than the one used here. That is why a numerical model was developed and used to model blister tests with different repair thicknesses.

In order to validate the numerical model using the blister test results obtained here, the test was initially simulated with a composite repair of 1.3 mm thickness. Figure 10 shows a good correlation between numerical and the experimental results. Especially in the Region 1, where the critical load is identified to determine the G_T and consequently to get the failure pressure. The CZM parameters were adjusted in order to fit the experimental results. The traction stress T and the interfacial displacement δ which best fit the results were 6 MPa and 0.03 mm, respectively. The critical load identified in this simulation was 582 N. According to equations 1 and 3, this critical load corresponds to exactly the same total energy release rate (G_T = 0.28 N/mm) and a failure pressure (100 Bar) found in the experimental blister test.

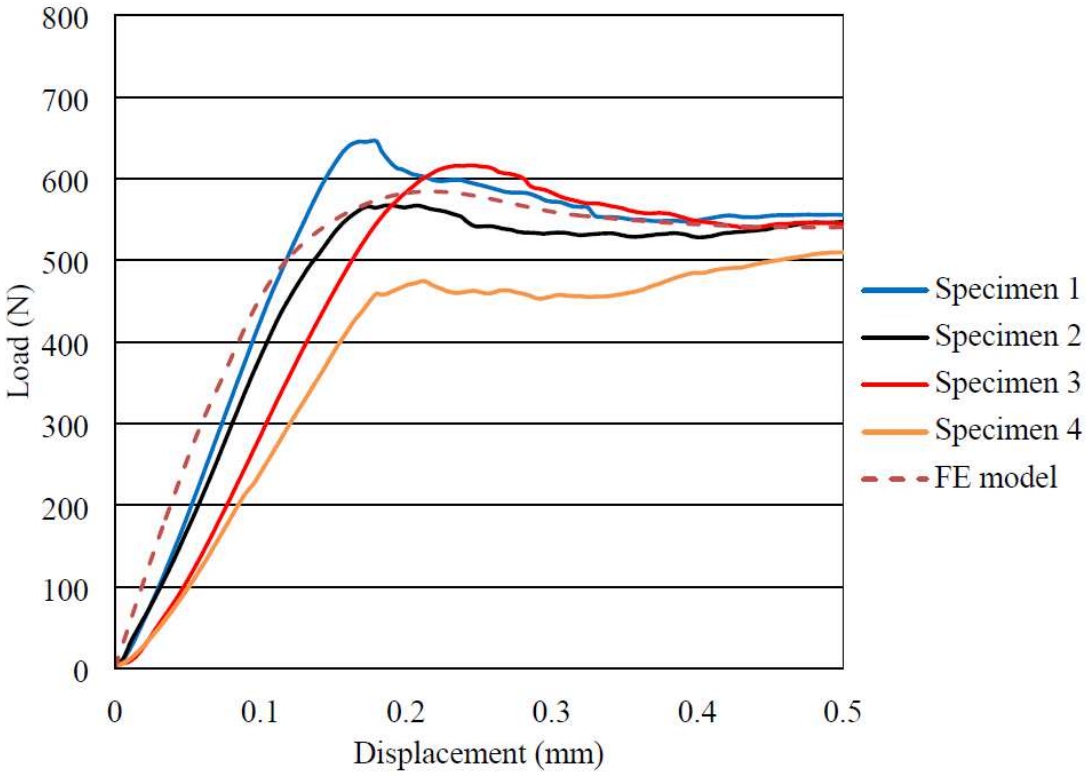

Figure 10. Load displacement curves in Region 1.

Since the validation of the FE model has been done, the model was used to investigate de influence of the repair thicknesses and the diameter of the hole in the critical load.

Figure 11 shows the load displacement curves obtained with four different composite repair thicknesses (t). In these simulations the hole diameter (d) was kept equal to 10 mm. It can be seen that, the repair thickness plays an important role in the onset debonding force, where the increase in the thickness leads to the increase in the debonding force. It is also important to notice that the critical force becomes unclear, as the repair thickness increases.

The shape of the load displacement curves also depends on the diameter of the hole, as can be seem in Figure 12. In these simulations repair thickness (t) was kept equal to 1.3 mm. With the increasing of the hole diameter, the debonding force increases as well, but here the point of the first debonding becomes more and more distinguishable when the diameter of the hole increases.

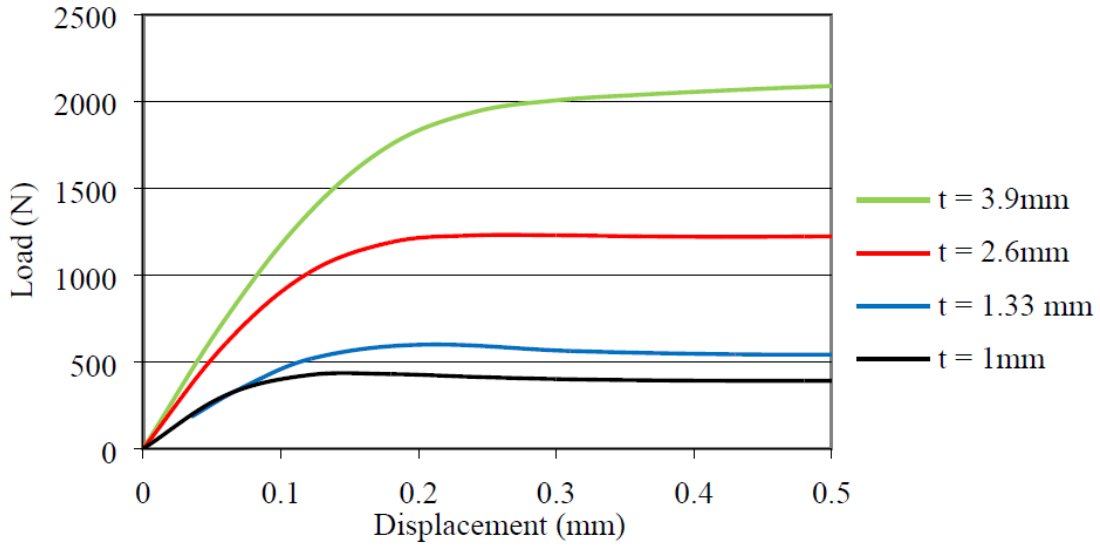

Figure 11. Load displacement curves with four different composite repair thicknesses.

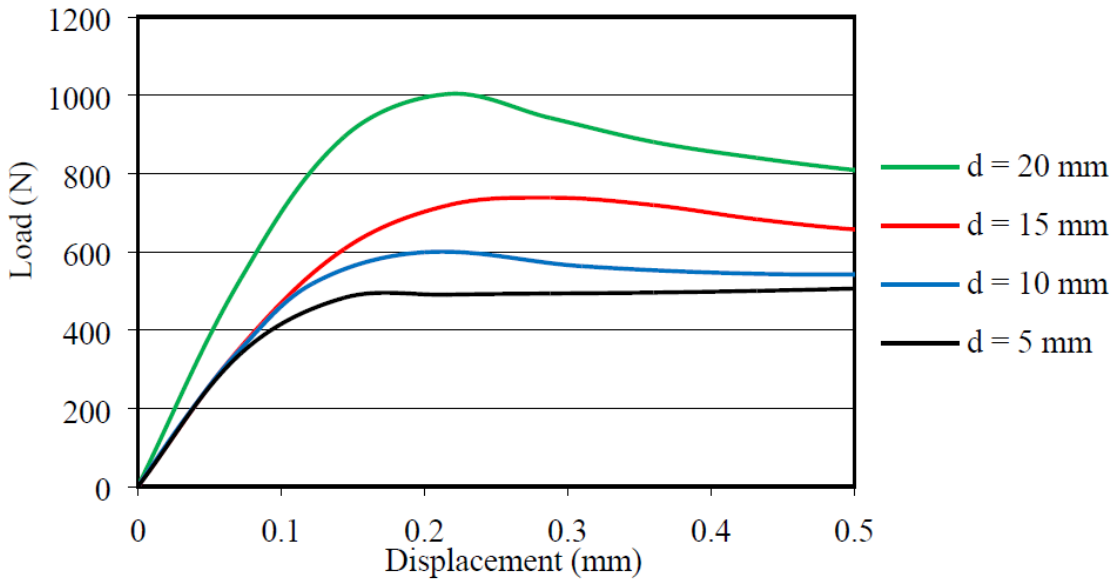

Figure 12. Load displacement curves with four different hole diameters.

Simulations with different values for the CZM parameters were performed in order to investigate the influence of the traction stress T and the interfacial displacement δ on the critical load. The Figure 13 presents the load displacement curves obtained when keeping δ equal to 0.03 mm and Figure 14 presents the results obtained when keeping T equal to 6 MPa.

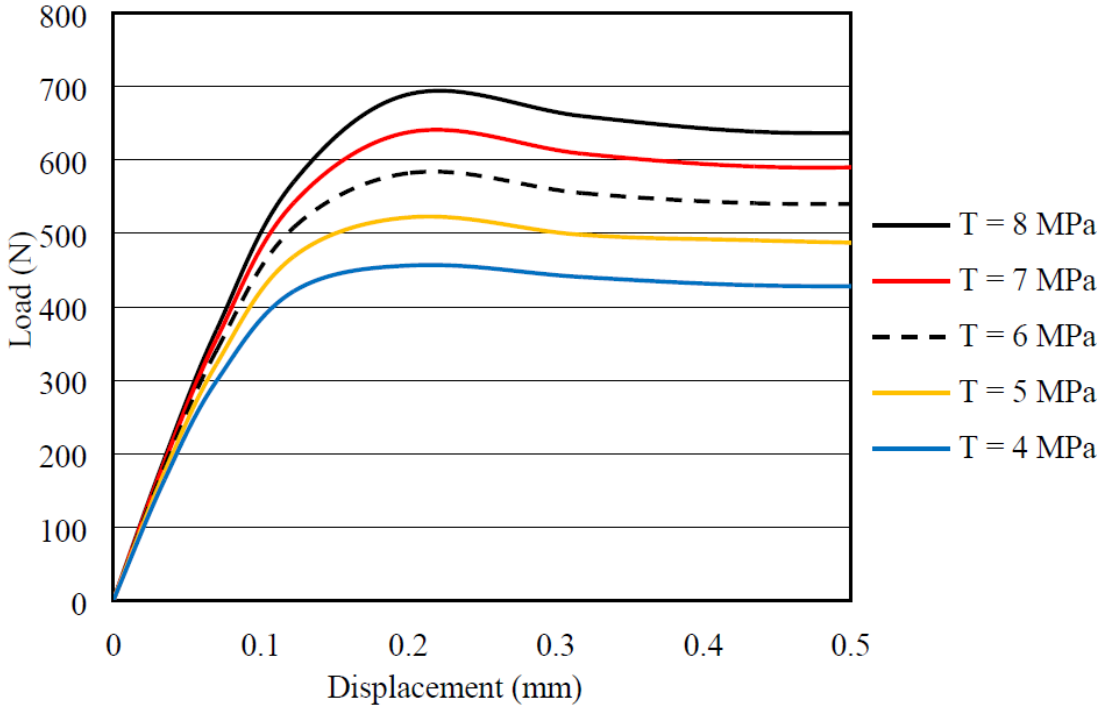

Figure 13. Influence of the parameter T in the critical load.

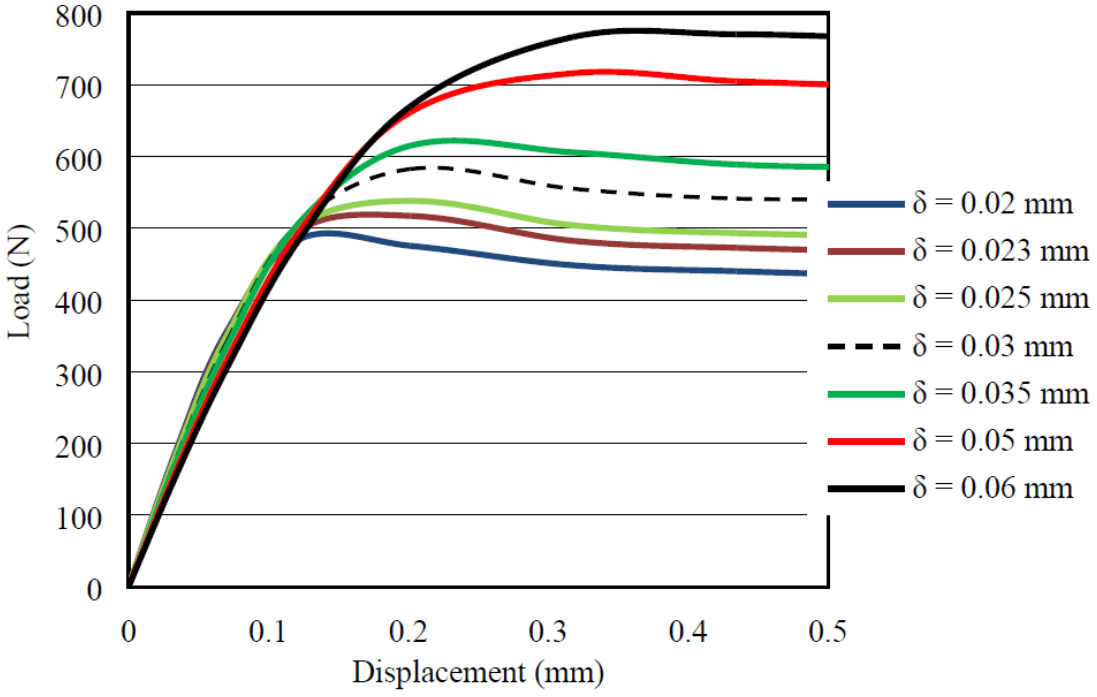

Figure 14. Influence of the parameter δ in the critical load.

The Table 4 compiles the critical load values taken from curves on Figures 13 and 14. It also presents the correspondent values for G_T and the failure pressure, calculated according to equations 1 and 3, respectively. The differences (Δ) between the values of critical load, G_T and failure pressure when compared to the ones obtained using T = 6 MPa and δ = 0.03 mm are also presented in separated columns.

Considering the standard deviation of the blister test as a reference (see Table 3), critical loads with a difference (Δ) less than 75 N could not be identified by this test. It means that, for a hole diameter of 10 mm and a repair thickness of 1.3 mm, the blister test is able to identify differences of G_T of the order of 0.07 N/mm (yellow values in Table 4), which is a very good sensibility. In a similar work, Alnaser and Keller [27] have used Width Tapered Double Cantilevered Beam (WTDCB) tests for obtaining critical fracture energy value than assess the failure pressure by using the eq. 3. They presented G_T values that reach variation ten times greater than the ones found here for the blister test (□0.78 N/mm).

In what concerns the failure pressure, the standard deviation of the blister test corresponds to a variation of about 1.16 MPa, which is in the same order that can be found for hydrostatic tests [27,30]. However, the onset debonding pressure is sometimes more difficult to identify during hydrostatic tests. In these tests, the failure pressure is often considered the pressure measured when oil leakage is identified which is not correct because the debonding starts before the complete failure of the repair. It means that blister test could replace hydrostatic tests with accuracy and some advantages, namely the easiest realization.

Table 4 – Total energy release rate (GT) and failure pressures.

T (MPa)	δ (mm)	F (N)	ΔF (N)	G_T (N/mm)	ΔG_T (N/mm)	P (MPa)	ΔP (MPa)
4	0.03	456	126	0.17	0.11	8.10	2.24
6	0.02	485	97	0.20	0.09	8.61	1.73
6	0.023	517	65	0.22	0.06	9.18	1.16
5	0.03	522	60	0.23	0.06	9.27	1.07
6	0.025	538	44	0.24	0.04	9.56	0.79
6	0.03	582	0	0.28	0.00	10.34	0.00
6	0.035	615	32	0.31	0.03	10.92	0.58
7	0.03	638	56	0.34	0.06	11.33	0.99
6	0.04	647	64	0.35	0.07	11.49	1.15
8	0.03	690	108	0.40	0.11	12.25	1.91
6	0.06	770	188	0.49	0.21	13.68	3.34

The hydrostatic tests results are presented in Table 5 together with the results obtained for the simulation of blister test with similar conditions. The first simulation performed took into account a diameter of 15 mm for the hole. The CZM parameters were adjusted according to these new conditions in order to get the critical load value correspond to the average failure pressure of 19.4 MPa obtained in the hydrostatic tests. The traction

stress T and the interfacial displacement δ which best fit this result were 14 MPa and 0.03 mm, respectively, corresponding to a failure pressure of 18.9 MPa according to Eq. 3. Then the other two geometric situations were simulated keeping the same values for the CZM parameters and the failure pressures calculated were very close to those found during the experimental test, as showed in Table 5.

Table 5 failure pressure results with the same repair thickness

d (mm)	t (mm)	P (Mpa) Experimental	F (N)(Model)	P (MPa)(Model) [Eq.3]
10	5.6	25.5	4500	22.4
15	5.6	19.4	4992	18.9
25	5.6	15.9	7180	17.1

As showed at Figures 9 and 10, the repair thickness and the diameter of the hole are the main geometrical parameters influencing the critical load and, consequently, in the failure pressure. In order to compare numerical results with hydrostatic test results with different repair thicknesses, new simulations were performed with the same test conditions presented in Rohen et al, 2016 [30]. Table 6 shows three experimental results for hydrostatic tests published in this former work. It is important to notice that the repair thickness varies according to the hole diameter. The first simulation performed took into account a diameter of 15 mm for the hole and a 2.2 mm thickness composite repair. The CZM parameters were adjusted according to these new conditions in order to get the critical load value correspond to the average failure pressure of 11.41 MPa presented in the previous work. The traction stress T and the interfacial displacement δ which best fit this result were 12 MPa and 0.02 mm, respectively, corresponding to a failure pressure of 11.99 MPa according to Eq. 3. Then the other two geometric situations were simulated keeping the same values for the CZM parameters and the failure pressures calculated were also very close to those found during the experimental test, as showed in Table 6.

Table 6 failure pressure results with different repair thickness

d (mm)	t (mm)	P (MPa) Experimental [REF.30]	F (N) (Model)	P (MPa) (Model) [Eq.3]
10	2	15.97	1125	14.99
15	2.2	11.41	1630	11.99
25	2.5	5.21	1922	6.17

The results presented in Tables 5 and 6 show once again that the blister test could replace hydrostatic tests for the analysis of the composite repairs performance.

4. Conclusion

In this work, prediction of failure pressure in bonded composite repaired pipes has been done by shaft-loaded blister tests. The energy release rate has been obtained by determining the interfacial debonding between the steel substrate and composite. The use of a steel half ball at the end of the shaft ensured an axisymmetric evolution of the blister shape which was monitored by DIC technique. A simple numerical model was used to investigate the accuracy of the blister test in terms of differences in failure pressure and energy release rate. A good correlation between the experimental and finite element simulation results has been obtained. The following conclusions were obtained from the analysis of test results and numerical simulations:

- Total energy release rate GT obtained from blister tests can be used to assess the repair failure pressure.
- The blister test is able to identify differences of 0.07 N/mm in the energy release rate GT and of 1.16 MPa in the failure pressure.
- Comparisons between numerical and hydrostatic test results showed that numerical model is able to identify the failure pressure for different hole diameters and repair thicknesses.
- These results show that the blister test could replace hydrostatic tests for the analysis of the composite repairs performance.

Acknowledgements

The authors would like to acknowledge the support of the Brazilian Research Agencies CNPq and FAPERJ.

References

1. Budhe S, Banea MD., de Barros S., da Silva LFM. An updated review of adhesively bonded joints in composite materials. Int J AdhesAdhes 2017; 72:30-42.

2. Budhe S., Bana M.D., Rohem N.R.F., Sampaio E.M., de Barros S. Failure pressure analysis of composite repair system for wall loss defect of metallic pipelines. Composite Structures. 2017; 176:1013-1019.

3. De Barros, S., Banea, M.D., Budhe, S., De Siqueira, C.E.R., Lobão, B.S.P., Souza, L.F.G. Experimental analysis of metal-composite repair of floating offshore units (FPSO). Journal of Adhesion, 2017. 93 (1-2), pp. 147-158.

4. Chan PH, Tshai KY, Johnson M, Li S. The flexural properties of composite repaired pipeline: numerical simulation and experimental validation. ComposStruct2015; 133:312–21

5. Nateche T, Hadj Meliani M, Khan SMA, Matvienko YG, Merah N, Pluvinage G. Residual harmfulness of a defect after repairing by a composite patch. Compos Struct 2015; 123:292–300.

6. Ochoa OO, Salama MM. Offshore composites: transition barriers to an enabling technology. Compos Sci Technol 2005; 65:2588–2596.

7. Alexander CR. Development of a composite repair system for reinforcing offshore risers, Ph.D. thesis, Texas A&M University; 2007.

8. Djukic LP, Hillier W, Eccleshall T, Falzon PJ, Leong KH, Leong AYL. A novel high pressure composite clamp for pipeline repair. In: Element oilfield engineering with polymers. Applied Market Information Ltd. (AMI) and Element; 2014.

9. Linden JM, Köpple M, Elder D, Gibson AG. Fracture mechanics of crack propagation in composite repairs of steel pressure piping. J Reinf Plast Composites. 2014; 33:526–532.

10. Lacombe R. Adhesion measurement methods: theory and practice. Florida: CRC Press, 2006.

11. Dannenberg H. Measurement of adhesion by a blister method. J Appl Polym Sci. 1961 ; 5 : 125-134.

12. Kendall K. Thin-film peeling – the elastic term. J. Phys. D: Appl. Phys. 1975; 8: 1449–1452.

13. Akono A.T., Ulm F.J. An improved technique for characterizing the fracture toughness via scratch test experiments.Wear2014; 313:117–124.

14. Evans A.G., Charles E.A. Fracture toughness determinations by indentation, J. Am. Ceram. Soc1976; 59: 371–372.

15. Jensen H.M. The blister test for interface toughness measurement. Eng. Fract.Mech1991; 40: 475–486.

16. Jensen H.M. Analysis of mode mixity in blister tests. Int. J. Fract 1998: 94 : 79–88.

17. Sofla A., Seker E., Landers J.P., Begley M.R. PDMS-glass interface adhesion energy determined via comprehensive solutions for thin film bulge/blister tests. J. Appl. Mech. 2010;77: 31007.

18. Malyshev B.M., Salganik R.L. The strength of adhesive joints using the theory of cracks, Int. J. Fract. Mech. 1965; 1:14–128.

19. Wang Y., Tong L. Closed-form formulas for adhesion energy of blister tests underpressure and point load. J. Adhes 2016; 92:171–193.

20. Kozlova M., Braccini O., Eustathopoulos N., Devismes M. F., Dupeux M. Shaft loaded blister test for metal/ceramic brazing fracture. Materials Letters 2008; 62: 3626–3628.

21. Linden J.M., Kotsikos G., Gibson A.G. Strain energy release rate in shaft-loaded blister tests for composite repairs on steel. Composites: Part A 2016; 81: 129–138.

22. Sun J.Y, Qian S.H., Li Y.M., He X.T., Zheng Z.L. Theoretical study of adhesion energy measurement for film/substrate interface using pressurized blister test. Energy release rate. Measurement 2013; 46: 2278–2287.

23. Mohammad S.I., Liyong T. Effects of initial blister radius and shaft diameter on energy release rate of metal–polymer composite coating. International Journal of Adhesion &Adhesives 2015; 62:107–123.

24. ISO/TS 24817:2017: Petroleum, petrochemical and natural gas industries. Composite repairs for pipework. Qualification and design, installation, testing and inspection. Standard; International Organization for Standardization, Geneva, Switzerland; 2017.

25. The American Society of Mechanical Engineers. ASME PCC-2-2015. Repair of pressure equipment piping; 2015.

26. Köpple M.F, Lauterbach S., Wagner W.Composite repair of through-wall defects in pipework – Analyticaland numerical models with respect to ISO/TS 24817. Composite Structures 2013;95: 173–178.

27. Alnaser I.A., Keller M.W., Comparison of coupon and full-scale determination of energy release rate for bonded composite repairs of pressure equipment. Engineering Fracture Mechanics 2015; 146: 31-40.

28. Alfano G., Crisfield M.A. Finite element interface models for the delamination analysis of laminated composites: mechanical and computational issues. Int. J. Numer. Meth. Engng. 2001; 50:1701-1736.

29. ASTM D1599: Standard test method for resistance to short-time hydraulic pressure of plastic pipe, tubing, and fittings; 2005.

30. Rohem N.R.F, Pacheco L.J., Budhe S., Banea M.D., Sampaio E.M., de Barros S. Development and qualification of a new polymeric matrix laminated composite for pipe repair. Composite Structures. 2016; 152 :737–745.